

# Model Membrane from Shed Snake Skins

M. Kumpugdee-Vollrath, T. Subongkot, T. Ngawhirunpat

## II. MATERIALS AND METHODS

**Abstract**—In this project we are interested in studying different kinds of shed snake skins in order to apply them as a model membrane for pharmaceutical purposes instead of human stratum corneum. Many types of shed snake skins as well as model drugs were studied by different techniques. The data will give deeper understanding about the interaction between drugs and model membranes and may allow us to choose the suitable model membrane for studying the effect of pharmaceutical products.

**Keywords**—DSC, FTIR, permeation, SAXS, shed snake skin.

### I. INTRODUCTION

THERE is a considerable interest in the use of alternative model membrane for *in vitro* pharmaceutical applications. However, it is particularly difficult to obtain human skin for *in vitro* experiments and it is therefore important to have alternative membranes which mimic human skin (Stratum corneum). The literature mentioned that membranes which can likewise be used are for examples pig skin [1] or reptile skin [2]. Especially the reptile skin from snakes appears to be a useful alternative to animal skin in assessing the potential for transdermal drug delivery because their behaviors are similar to that of human stratum corneum, in term of the thickness and the lipid composition [2]. The advantage of the reptile skin is that they change their skins regularly. Therefore it is not necessary to kill the animal or to isolate the stratum corneum from the reptile skin. Another advantage is that they are easy to handle as well as to storage and they can be obtained from a reptile shop or farm. However, the lack of hair follicles is the main difference between snake and human stratum corneum [2], [3]. Therefore the use of these alternative membranes in transdermal research has a certain limitation. In this project we are interested in studying different kinds of shed snake skins in order to apply them as model membrane for pharmaceutical purposes. Different techniques [4]-[6] (e.g. differential scanning calorimetry, Fourier Transform Infrared Spectroscopy, Small and Wide angle X-ray scattering, and permeation test) were therefore applied to understand the interaction between drugs and model membranes and may allow us to choose the suitable model membrane for testing of pharmaceuticals.

M. Kumpugdee-Vollrath is a professor at Beuth Hochschule für Technik Berlin - University of Applied Sciences, Faculty of Mathematics-Physics-Chemistry, Pharmaceutical and Chemical Engineering, Luxemburger Str. 10, D-13353 Berlin, Germany (phone (+4930) 4504-2239; Fax: (+4930) 4504-2813; e-mail: vollrath@beuth-hochschule.de)

T. Subongkot is a PhD student at Silpakorn University, Faculty of Pharmacy, Department of Pharmaceutical Technology, Nakhon Pathom, Thailand 73000, Thailand (e-mail: titanicto@hotmail.com).

T. Ngawhirunpat is associated professor at the Silpakorn University, Faculty of Pharmacy, Department of Pharmaceutical Technology, Nakhon Pathom, Thailand 73000, Thailand (e-mail: tanasait@su.ac.th).

### A. Materials

Different kinds of drugs were studied i.e. resveratrol (res), ketoprofen (ket), lidocaine HCl (lh), lidocaine base (lib), lignan (li), paracetamol (Pa), aspirin (As) and ibuprofen (Ib). Many types of shed snake skins were applied.

### B. Solubility Studies

The saturated solubility of each drug in ethanol-water mixture 50%v/v was determined. An example of preparation was explained by the drug ketoprofen as follows. Saturated solution of ketoprofen was prepared by adding excess amount of drug in a 10ml volumetric flask with a solvent mixture. The containers were sealed and stirred with magnetic stirrer (IKA, Germany) for 24h at ambient temperature. After 24h, the solution was filtered through filter paper. The supernatant was used for skin penetration study. For solubility measurement, the filtered saturated drug solution was diluted suitably and analyzed by ultraviolet spectrophotometer (UV/VIS Spectrophotometer JASCO V630, MD, USA) at the maximum wavelength of ketoprofen at 260nm. The solubility of ketoprofen was calculated by referring to a calibration curve obtained by using standard solutions of ketoprofen ranging from 2 to 10 µg/ml. The saturated solutions and solubilities of other drugs were determined in the same way. The maximum wavelength of each drug was as follows; res = 305nm, lh = 263nm, lib = 263nm, li = 279nm.

### C. Optical Determination

Photographs were taken with the digital camera (Nikon coolpix, Nikon Corporation, Japan) and the morphology was examined with a scanning electron microscope (SEM, Digital Scanning Microscope DSM 950, Zeiss, Germany) at a high voltage of 10 kV. Before measurement, samples were coated with a thin layer of gold-palladium in a SEM Coating Unit E 5000 (Polaron Sputter Coater, Polaron Instruments, UK).

### D. Differential Scanning Calorimetry (DSC)

The DSC thermograms of the different samples were observed by a Perkin Elmer DSC 7 (Perkin Elmer, Massachusetts, USA), which was calibrated with indium. The thermal behavior was studied by heating about 2-5mg sample in a sealed aluminum pan under nitrogen gas at the temperature range of 30-300°C using heating rates of 10°C/min. For skins which were treated with a drug, the saturated solution of each drug was prepared as mentioned in part B. Skins were stored in the saturated clear solution for 24h before they were taken out and washed many times with sterile water. Skins were dried by tissues and stored in a desiccator prior to measurement.

#### E. Attenuated Total Reflectance-Fourier Transform Infrared Spectroscopy (ATR-FTIR)

ATR-FTIR spectra were obtained using a Perkin-Elmer spectrophotometer (Spectrum 100, USA) equipped with a crystal diamond universal ATR sampling accessory. Before each measurement, the ATR crystal was carefully cleaned with acetone. During each measurement, the outer surface of the skin sample was in contact with the Universal diamond ATR top-plate. For each sample, the spectrum obtained represented an average of 4 scans recorded within the range of 4000–400 $\text{cm}^{-1}$  with a 4 $\text{cm}^{-1}$  resolution. Skins treated with a drug were prepared similar to that mentioned in part D.

#### F. Small and Wide Angle X-Ray Scattering (SWAXS)

The experiments were performed with small and wide angle X-ray scattering (SAXS and WAXS) instrument, beamline B1, installed at the DORIS III synchrotron source at HASYLAB/DESY in Hamburg, Germany. SAXS scattering patterns (0–1 Å) were acquired using a large area pixel detector (PILATUS 1 M, Dectris, Switzerland) with a pixel size of 172 $\mu\text{m}\times 172\mu\text{m}$ . WAXS (1–4 Å) was measured simultaneously using a Mythen strip detector (Dectris, Switzerland). The distance from the sample to detector was 0.885m, and the X-ray energy was 14 keV. Samples of both parts (hinge and scale areas) of the model membrane were folded 4–5 times (about 4 $\times$ 4 mm) and fixed onto a holder, which was then placed into a vacuum chamber and measured for SWAXS. The raw scattering data were background corrected, integrated and calibrated using a MATLAB-based analysis suite, which is available at the beamline. Peak positions were determined by using Origin software to fit a Gaussian equation to the data. Considering the lamellar phase of the lipid determined by the Bragg equation, the repeat distance or the length of the unit cell “d” was calculated as follows;

$$d = \frac{2n\pi}{q_n} \quad (1)$$

where n=the order of the diffraction peak, and  $q_n$ =scattering vector at the particular order.

Skins treated with a drug were prepared similar to that mentioned in part D.

#### G. Permeation Test

The skin penetration study of five different drugs (i.e. ketoprofen, resveratrol, lidocaine HCl, lidocaine base, and lignan) through shed snake skins was performed using Franz diffusion cells with a penetration area of 0.785 $\text{cm}^2$ . The receiver compartment was filled with 5ml of distilled water, stirred with a magnetic bar at a rate of 500rpm. The shade snake skin was mounted in between the diffusion chamber of the cell (Fig. 1). Diffusion cells were connected with a circulating water bath to maintain the temperature at 32°C. This temperature is similar to that of human skin. Two hundred microliters of the saturated drug solution was placed into the donor compartment. At the predetermined times of 1, 2, 4, 6, 8 and 24h, three hundred microliters of sample were

taken by a syringe and put into a micro sized plastic cuvette (microsized UV-Transparent Disposable Cuvette, BrandTech Scientific Inc, Germany). The sample was detected in 2 replicates using an UV spectrophotometer. The skin penetration kinetics of drugs was investigated using the zero-order model as well as the Higuchi model as follows;

#### 1. Zero Order Model

The data obtained from in vitro skin penetration studies were plotted between cumulative amounts of drug permeated vs. time. This model shown in (2), describes the drug release pattern assuming that the drug release rate is independent of its concentration;

$$Q = k_0t \quad (2)$$

where Q is the amount of drug permeated in time t,  $k_0$  is the zero order constant expressed in units of concentration/time, and t is time.

#### 2. Higuchi Model

This model describes drug release from a matrix system as a process that is dependent on the square root of time, based on Fickian diffusion as shown in (3);

$$Q = K t^{1/2} \quad (3)$$

where Q is the cumulative amount of drug permeated in time  $t^{1/2}$ , K is the Higuchi rate constant, and  $t^{1/2}$  is the square root of time. A straight line could be obtained from plotting between Q and  $t^{1/2}$ . The resultant slope is the Higuchi rate constant.

#### H. Data and Statistic Analysis

The cumulative amount of drug penetrating through the shed snake skin per unit area was plotted as a function of time. The flux (J) and lag time were determined from the slope and the x-intercept of the linear portion, respectively. The permeability coefficient ( $K_p$ ) was calculated by:

$$K_p = J/\text{Conc} \quad (4)$$

where J is the flux of drugs penetrated through shade snake skin of *Python molurus molurus*. Conc is the drug concentration in donor part. All data was statistically analyzed by analysis of variance (ANOVA), followed by the LSD post hoc test. Differences of  $p < 0.05$  were considered statistically significant and expressed as \*.

### III. RESULTS AND DISCUSSION

#### A. Solubilities and Calibrations

The calibrations of five drugs were successfully performed because every drug could absorb the UV and had the suitable maximum absorptions. Examples of calibrations of a drug in different media (i.e. water, mixture of water and ethanol) were shown in Fig. 2. The slopes have a small difference, which should be considered in the calculation. Table I shows the summarization of all calibration curves and equations. The

drug amount and solubilities can be calculated by the respective equation. The solubilities of drugs were demonstrated in Tables IV and V.



Fig. 1 Photograph of Franz Diffusion cell with a shed snake skin in between the donor and receptor parts

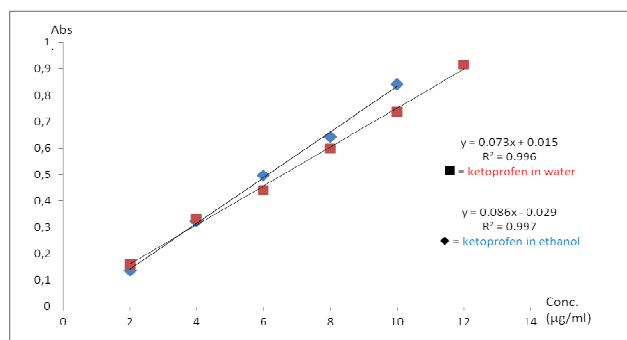


Fig. 2 Calibration curve of ketoprofen in water and in water-ethanol (50:50%) at 260 nm

TABLE I

SUMMARY OF ALL CALIBRATION CURVES WITH CALIBRATION EQUATIONS

Type of drug	Calibration's Equation	R <sup>2</sup>
Ketoprofen in water	Y=0.073x-0.015	0.996
Ketoprofen in 50% ethanol	Y=0.086x-0.029	0.997
Resveratrol in water	Y=98.75x-0.019	0.997
Resveratrol in 50% ethanol	Y=0.112x	0.994
Lidocaine HCl in water	Y=0.001x-0.021	0.996
Lidocaine HCl in 50% ethanol	Y=0.002x-0.153	0.997
Lidocaine in water	Y=0.001x+0.014	0.994
Lidocaine in 50% ethanol	Y=0.001x-0.074	0.993
Lignan in water	Y=0.008x-0.018	0.994
Lignan in 50% ethanol	Y=0.008x-0.151	0.999

### B. Optical Determination

Examples of the optical results were shown in Fig. 3. The hinge and scale-regions of shed snake skin can be well seen. The color of *Python molurus* was brighter than the others but the scale sizes were almost the same. Fig. 4 shows SEM of different shed snake skins. The structure of scale and hinge was almost similar if we focused the two regions at the high magnifications [7].

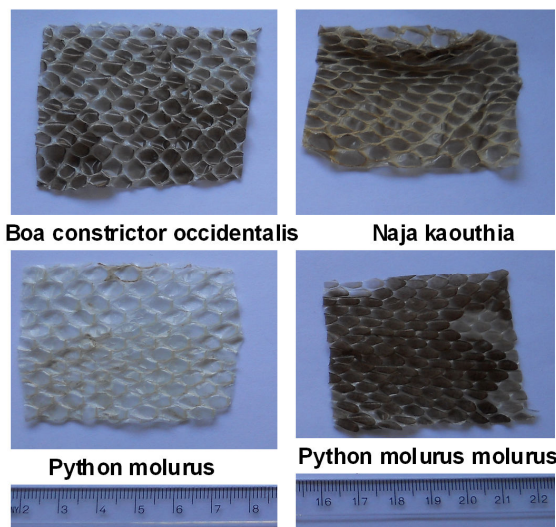


Fig. 3 Photographs of different types of shed snake skins

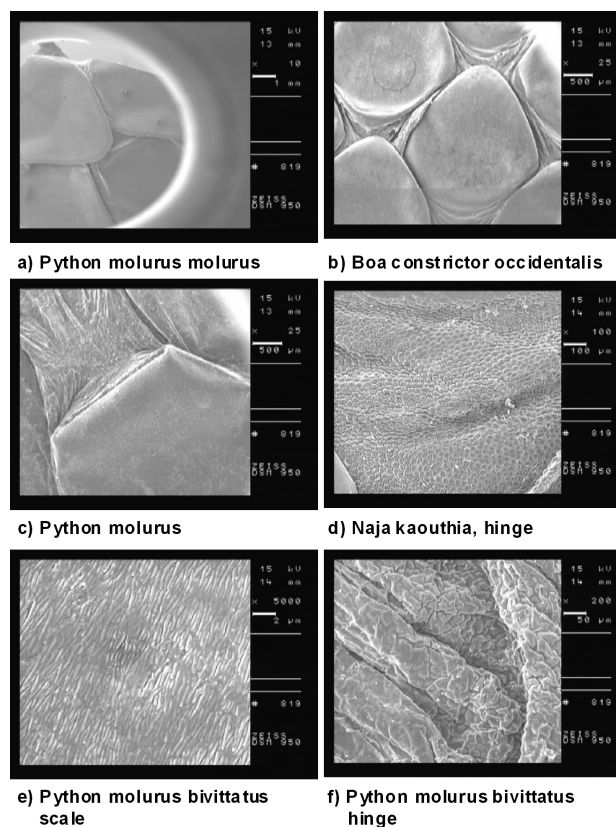


Fig. 4 SEM of different types of shed snake skins

### C. DSC

The melting point or transition temperature of a drug and of the shed snake skin can be monitored by the DSC. Examples of DSC thermograms of some shed snake skins can be seen in Fig. 5. The significant transition peaks of skins appear in the region of 55-60°C, but there was no difference between tested shed snake skins. Fig. 6 shows examples of some DSC-thermograms of pure drug and skins treated with a drug. The melting point of a pure drug showed a sharp peak. An example

is shown in Fig. 6 (A). The melting point of paracetamol can be clearly seen at 169.97°C, the onset was 168.21°C. After the shed snake skin (i.e. *Python molurus molurus* = pmm) was treated with paracetamol or lignan, the melting peaks showed at higher temperatures i.e. 178°C and 222°C, respectively. In contrast, if the shed snake skins (i.e. *Boa constrictor occidentalis* = bco) were treated with aspirin, the melting peak get lower from 142°C to 129°C.

Table II summarizes the melting peaks of the pure drug or shed snake skin treated with a drug. Only the peak of a drug was monitored and showed in the table. If no peak of drug can be detected, the transition peak of the skin was shown. The data showed that ibuprofen peak was not found after the skins were treated with ibuprofen and measured. This means that ibuprofen cannot penetrate into the shed snake skin. On the other hand, other drugs e.g. aspirin, paracetamol and lignan can penetrate into the skins. These drugs seemed to change the structure of the skins because the melting peaks of drugs were changed (both increase and reduce) compared to the pure drug.

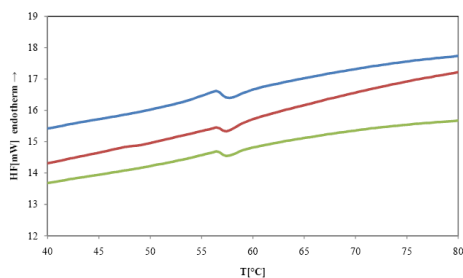


Fig. 5 DSC-thermograms of *Python molurus molurus* (blue), *Python molurus bivittatus* (red), and *Naja kaouthia* (green)

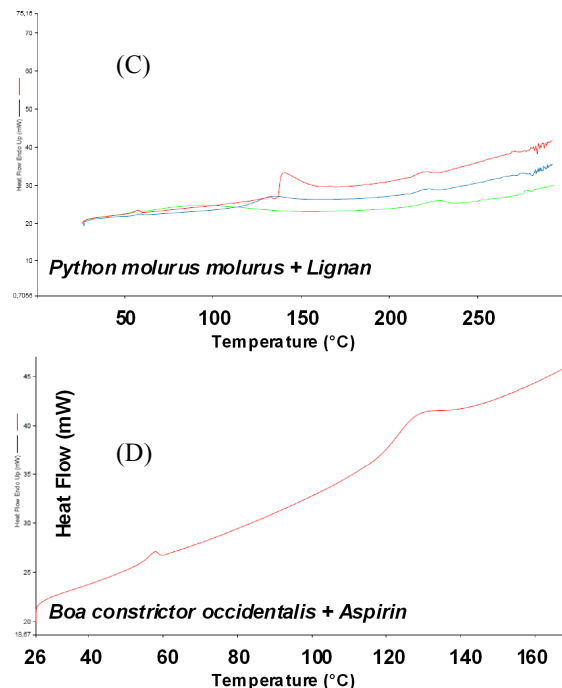
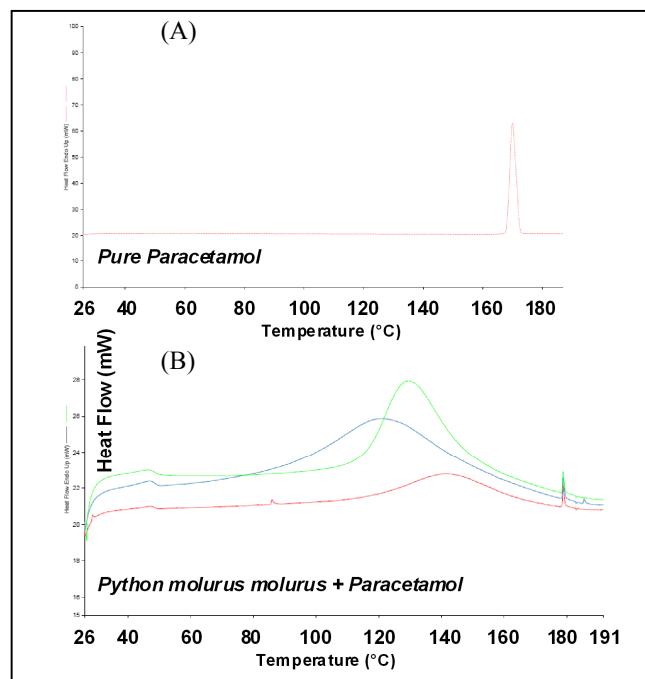


Fig. 6 DSC-thermograms of (A) pure paracetamol, (B) *Python molurus molurus* treated with paracetamol or (C) *Python molurus molurus* treated with lignan and (D) *Boa constrictor occidentalis* treated with aspirin.

TABLE II  
 SUMMARY OF DSC RESULTS SHOWING THE MELTING PEAKS (°C, MEAN) OF PURE DRUG OR SHED SNAKE SKINS TREATED WITH A DRUG (N= 1 TO 3, SD= STANDARD DEVIATION)

Drug (+ Skin)	Temperature (Mean, °C)	Temperature (SD, °C)
Ibuprofen	76.61	0.50
Ib+ <i>Python molurus</i>	56.75	0.63
Ib+ <i>Python molurus molurus</i>	56.94	0.54
Ib+ <i>Boa constrictor occidentalis</i>	58.28	0.62
Ib+ <i>Elaphe schrenki</i>	58.70	0.13
Ib+ <i>Naja kaouthia</i>	55.34	
Aspirin	142.33	0.61
As+ <i>Python molurus</i>	127.33	
As+ <i>Python molurus molurus</i>	135.81	
As+ <i>Boa constrictor occidentalis</i>	128.62	
As+ <i>Elaphe schrenki</i>	131.07	0.82
As+ <i>Naja kaouthia</i>	134.23	2.47
Paracetamol	170.80	0.79
Pa+ <i>Python molurus</i>	178.76	0.01
Pa+ <i>Python molurus molurus</i>	178.76	0.01
Pa+ <i>Elaphe schrenki</i>	178.74	0.01
Pa+ <i>Naja kaouthia</i>	178.74	
Lignan	211.67	2.45
Lignan+ <i>Python molurus</i>	227.45	3.75
Lignan+ <i>Python molurus molurus</i>	222.91	3.93
Lignan+ <i>Boa constrictor occidentalis</i>	223.47	4.36
Lignan+ <i>Elaphe schrenki</i>	222.07	2.93
Lignan+ <i>Naja kaouthia</i>	221.60	4.34
Pure <i>Python molurus</i>	57.21	0.28

#### D. SWAXS

Fig. 7 shows a typical SWAXS pattern of different types of shed snake skins with two typical peaks at the region of 0.2-2.0 Å<sup>-1</sup>. There was no significant different peak, which means all tested shed snake skins give almost similar X-ray scattering pattern. The orientation of lipids and proteins inside the skins should be the same. The lamellar structure can be calculated by (1).

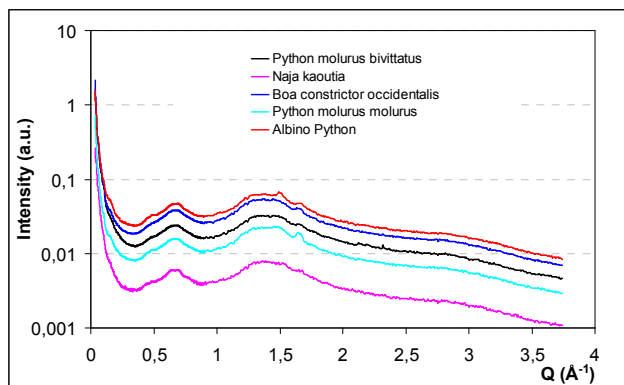


Fig. 7 SAXS-WAXS of different types of shed snake skins

#### E. FTIR

Fig. 8 shows the FTIR-spectra of different kinds of skins. There are small differences in the region which are marked by red lines. Wavenumbers in the region of 1300-1500 cm<sup>-1</sup> represented the chemical bond of C-C, C-O, C-N or double bond of them or even N=O. This may indicate that the chemical substances i.e. lipids or proteins inside the shed snake skins may differ or have different amount between species. After the shed snake skins were treated with different drugs (Fig. 9), the small changes in the same region were observed, which means that the chemical bonding between substances may change [8].

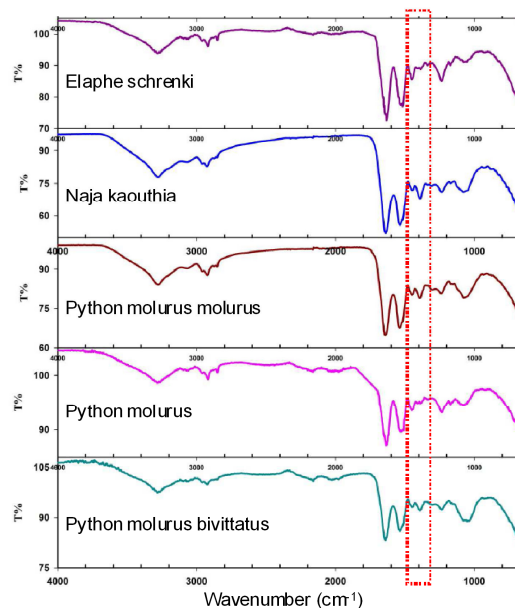


Fig. 8 FTIR-Spectra of different shed snake skins without treatment

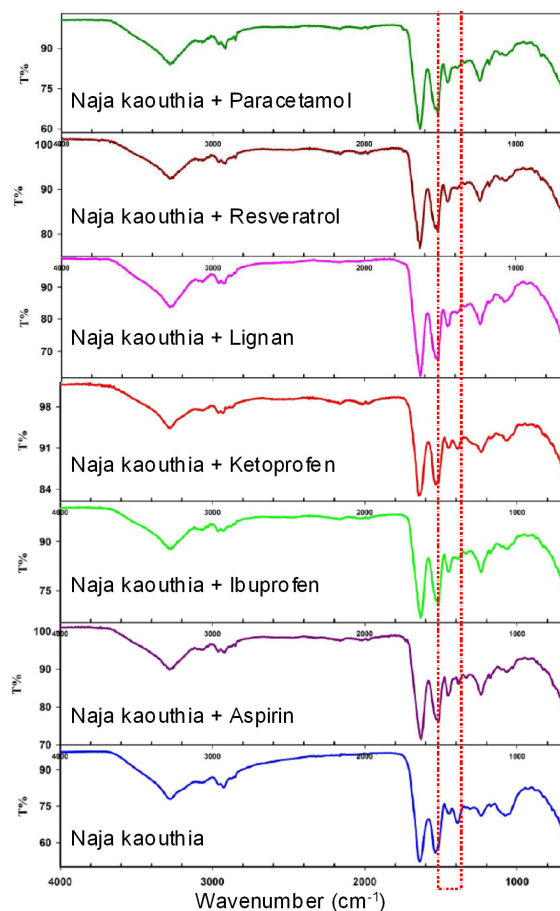


Fig. 9 FTIR-Spectra of shed snake skin *Naja kaouthia* treated with different drugs

#### F. Permeation Test

The summary of the skin permeation of saturated ketoprofen in 50%v/v ethanol in water can be seen in Fig. 10

and Table III. Fig. 10 shows that the fluxes were not significantly different at the sampling times. Table III shows that the lag time of skin "*Boa constrictor occidentalis*" was significant different from the others. This may be due to the lipids and proteins in the skins, which may differ from the other skins. This hypothesis should be confirmed in the future studies.

Because of the fact that tests by DSC, FTIR and SWAXS did not show significant differences between the shed snake skins and as the permeation test with ketoprofen showed only small differences between skins, we have chosen skins from *Python molurus molurus* for further permeation test with different drugs.

The permeation tests of resveratrol and lignan were shown in Fig. 11. As the drug permeation of lidocaine HCl and lidocaine base was in milligram, therefore the graph was separately demonstrated in Fig. 12. Tables IV and V show all results of five tested drugs. Lag times of ketoprofen and resveratrol were significant difference and permeation coefficient of lidocaine had the lowest value compared between those five drugs. Flux values cannot be directly compared because they depended on the concentrations in the donor part, which were different. Various drugs have different effects on the skin, which may be due to their physical chemical properties [5], [9], [10]. Therefore the values were summarized in the Table VI. We have found that the permeation did not only depend on the solubility but also on other values e.g. pKa, molecular weight and therefore caused complicated permeation profile. Further studies to find the correlation between these parameters will be performed in the future experiments.

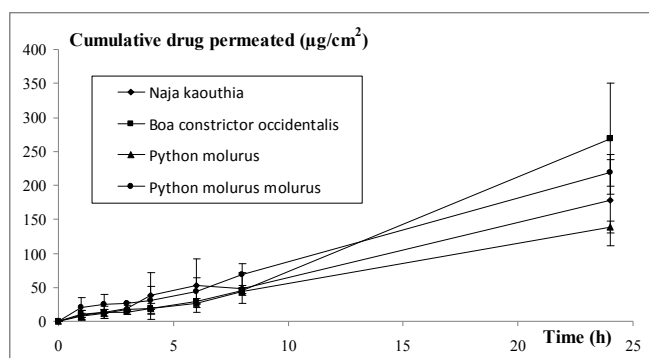


Fig. 10 Permeability curves of ketoprofen through four types of shed snake skins

TABLE III

SUMMARY OF IN VITRO SKIN PENETRATION STUDY OF SATURATED KETOPROFEN IN 50 % V/V ETHANOL THROUGH FOUR TYPES OF SHED SNAKE SKINS

Type of shade snake skin	Flux ( $\mu\text{g}/\text{cm}^2/\text{h}$ )	Lag time (h)
<i>Boa constrictor occidentalis</i>	8.67 $\pm$ 1.54	2.11 $\pm$ 0.75*
<i>Naja kaouthia</i>	6.40 $\pm$ 1.00	0.67 $\pm$ 0.53
<i>Python molurus</i>	5.63 $\pm$ 0.32	0.47 $\pm$ 0.14
<i>Python molurus molurus</i>	8.98 $\pm$ 0.99	1.08 $\pm$ 0.25

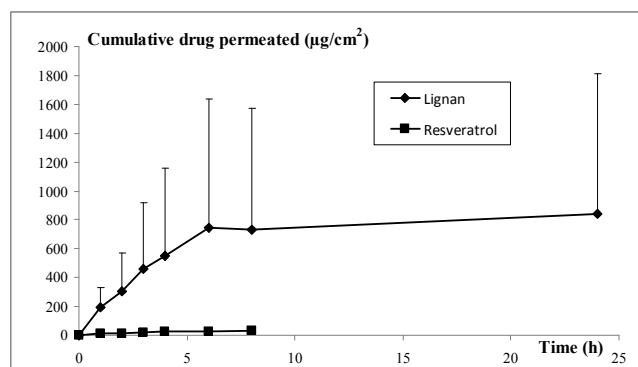


Fig. 11 Permeability curves of lignan and resveratrol through *Python molurus molurus*

TABLE IV  
RESULTS OF IN VITRO SKIN PENETRATION STUDY OF KETOPROFEN, RESVERATROL AND LIGNAN (IN  $\mu\text{G}$ ) THROUGH *PYTHON MOLURUS MOLURUS*

Type of drug	Solubility in 50% EtOH (mg/ml)	Flux ( $\mu\text{g}/\text{cm}^2/\text{h}$ )	Lag time (h)	$K_p$ ( $\text{ml}/\text{cm}^2/\text{h}$ )
Ketoprofen	55.81	8.98 $\pm$ 0.99	1.08 $\pm$ 0.25*	0.00016 $\pm$ 0.000
Resveratrol	23.41	9.49 $\pm$ 6.82	0.15 $\pm$ 0.04*	0.00040 $\pm$ 0.000
Lignan	209.02	323.3 $\pm$ 441.7	0.63 $\pm$ 0.72	0.00154 $\pm$ 0.002

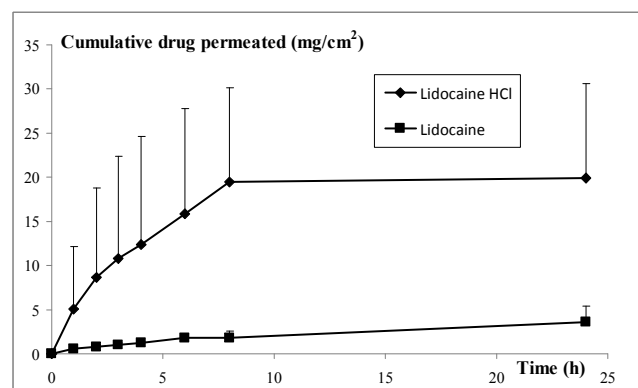


Fig. 12 Permeability curves of lidocaine HCl and lidocaine base through *Python molurus molurus*

TABLE V  
RESULTS OF IN VITRO SKIN PENETRATION STUDY OF LIDOCAINE HCL AND LIDOCAINE BASE (IN MG) THROUGH *PYTHON MOLURUS MOLURUS*

Type of drug	Solubility in 50% EtOH (mg/ml)	Flux ( $\text{mg}/\text{cm}^2/\text{h}$ )	Lag time (h)	$K_p$ ( $\text{ml}/\text{cm}^2/\text{h}$ )
Lidocaine HCl	677.3	7.65 $\pm$ 1.85	0.83 $\pm$ 0.24	0.01129 $\pm$ 0.0027
Lidocaine	0.585	0.79 $\pm$ 1.00	0.52 $\pm$ 0.19	1.35043 $\pm$ 1.7094*

All tables with  $p < 0.05$ , \* shows significant difference  
Each value represents the mean $\pm$ SD (n=3)  
 $K_p$  = Permeability coefficient (Flux/solubility)

TABLE VI  
PHYSICO-CHEMICAL PROPERTIES OF DRUGS USED FOR SKIN PENETRATION  
STUDIES; MW = MOLECULAR WEIGHT, NN = NOT FOUND

Type of drug	Log P	pKa	MW
Ketoprofen	3.12[11], 0.97[13]	4.6 (weak acid)[11] , 4.76[12]	254.28
Resveratrol	3.1[14],[16]	1. the pKa values of <i>trans</i> -resveratrol corresponding to the mono, di- and tri-protonation of the system were 9.3, 10.0 and 10.6[17] 2. pKa1 = 8.8, pKa2 = 9.8, pKa3 = 11.4 of (E)-resveratrol in aqueous medium[18]	228.24
Lidocaine HCl	Log P <0[15]	7.16[18]	270.8
Lidocaine base	2.4, 2.6[15]	7.8[19]	234.34
Lignan (secoisolaricir esinol diglucoside)	NN	NN	686.7

TABLE VII  
R<sup>2</sup> OF LINEAR REGRESSION OF RELATIONSHIP BETWEEN CUMULATIVE DRUG PERMEATED THROUGH *PYTHON MOLURUS MOLURUS* AND TIME

Type of drug	R <sup>2</sup> of Zero order	R <sup>2</sup> of Higuchi
Ketoprofen	0.990	0.762
Resveratrol	0.644	0.987
Lidocaine HCl	-0.230	0.982
Lidocaine base	0.787	0.975
Lignan	-0.170	0.957

The calculations in Table VII were performed only in the time period of 0-8h. It can be seen that the release of ketoprofen followed the Zero order model, whereas other drugs followed the Higuchi model.

#### IV. CONCLUSION

By application of different techniques we have seen that different kinds of shed snake skins have only small variation from each other. These results may indicate that most of the shed snake skins can be used as a model membrane for pharmaceutical purposes. In order to select the suitable model membrane, we recommend to take a skin which can be most easily found in the own region. For our purpose the skin from *Python molurus molurus* was most effective because we can easily get it from the reptile shop without any cost. The storage can be easily done in the room temperature or in the refrigerator. Various drugs have different effects on the skin, which may also be due to the physical chemical properties of each drug. Further studies should be performed to get more understanding about the correlation between parameters.

#### ACKNOWLEDGMENT

The authors would like to thank S. Braun, R. Trummer, G. Ahmadi, and H. Bilek for performing experiments, Prof. Dr. H. Hungerbühler and E. Leo for the DSC measurements, J. Landskron for the SEM-measurements, DESY, Beamline B1 and Dr. U. Vainio for the SWAXS-measurements, as well as the European Regional Development Fund (ESF), Zentrales Innovationsprogramm Mittelstand (ZIM), the Federal ministry

of Economics and Technology (BMW) of Germany, and the Thailand Research Funds through the Golden Jubilee Ph.D. Program for the financial support.

#### REFERENCES

- [1] T. Ngawhirunpat, P. Opanasopit, S. Prakongpan, Comparison of skin transport and metabolism of ethyl nicotinate in various species. *Eur J Pharm Biopharm*, 2004, 58(3), 645-51.
- [2] T. Ngawhirunpat, S. Panomsuk, P. Opanasopit, T. Rojanarata, T. Hatanaka, Comparison of the percutaneous absorption of hydrophilic and lipophilic compounds in shed snake skin and human skin. *Pharmazie*, 2004, 61(4), 331-5
- [3] T. Itoh, J. Xia, R. Magavi, T. Nishihata, H. Rytting, Use of shed snake skin s model membrane for percutaneous absorption studies; comparison with human skin. *Pharmaceutical Research*, 1990, 7(10), 1042-7.
- [4] N. Wonglertnirant, T. Ngawhirunpat, M. Kumpugdee-Vollrath, Evaluation of skin enhancing mechanism of surfactants on the biomembrane from shed snake skin, *Biological & Pharmaceutical Bulletin*, 2012, 35(4), 1-9.
- [5] A. Nasedkin, J. Davidsson, M. Kumpugdee-Vollrath, Determination of nanostructure of liposomes containing two model drugs by X-ray scattering from a synchrotron source, *Journal of Synchrotron Radiation*, 2013, 20, 721-728.
- [6] H. Bilek, N. Wonglertnirant, T. Ngawhirunpat, P. Opanasopit, M. Kumpugdee-Vollrath, Effect of terpenes on the skin permeation of ketoprofen through shed snake skin, *Silpakorn University Science and Technology Journal*, Silpakorn University Publisher, 2009, 3 (2), 33-41.
- [7] H. Bilek, M. Kumpugdee Vollrath, *Entwicklung Transdermaler Drug Delivery Systeme, Nachhaltige Forschung in Wachstumsbereichen Band II*, Beuth Hochschule für Technik, Logos Verlag Berlin, 2011, 15-20.
- [8] G. Ahmadi, *Physikalisch - chemische Untersuchungen von Modellmembranen am Beispiel abgeworfener Schlangenhäute*, Bachelor-Thesis, Beuth Hochschule für Technik Berlin - University of Applied Sciences, Berlin, Germany, 2013.
- [9] A. Naik, Y. N. Kalia, R. H. Guy, *Transdermal drug delivery: overcoming the skin's barrier function*, PSTT, 2000, 3 (9), 318-326.
- [10] H. A. E. Benson, *Transdermal Drug Delivery: Penetration Enhancement Techniques*, *Current Drug Delivery*, 2005, 2, 23-33.
- [11] P. N. Craig, In *Comprehensive Medicinal Chemistry*, C. Hansch, P. G. Sammes, J. B. Taylor, Eds., Pergamon: New York, 1990, Vol. 6.
- [12] J.J. Sheng, N.A. Kasim, R. Chandrasekharan, G.L. Amidon, Solubilization and dissolution of insoluble weak acid, ketoprofen: Effects of pH combined with surfactant, *Eur. J. Pharm.*, 2006, 306-314.
- [13] E. Beetge, J. du Plessis, D.G. Muller, C. Goosen, F.J. van Rensburg, The influence of the physicochemical characteristics and pharmacokinetic properties of selected NSAID's on their transdermal absorption, *Int. J. Pharm.*, 2000, 261-264.
- [14] <http://www.chemaxon.com/products/calculator-plugins/property-predictors/#pka> cited on 18 September 2013
- [15] <http://www.sciencedirect.com/science/article/pii/S0378517310004163> cited on 18 September 2013
- [16] M. Deak, H. Falk, On the chemistry of resveratrol diastereomers. *Monat fur Chem*, 2003, 134, 883-888.
- [17] J. M. López-Nicolás, F. García-Carmona, Aggregation State and pKa Values of (E)-Resveratrol As Determined by Fluorescence Spectroscopy and UV-Visible Absorption, *J. Agric. Food Chem.*, 2008, 56 (17), 7600-7605.
- [18] H. Sjöberg, K. Karami, P. Beronius, L. Sundelof, Ionization conditions for iontophoretic drug delivery. A revised pKa of lidocaine hydrochloride in aqueous solution at 25°C established by precision conductometry, *Int. J. Pharm.*, 1996, 141, 63-70.
- [19] [http://www.ifna-int.org/ifna/e107\\_files/downloads/lectures/H1LocalAne.pdf](http://www.ifna-int.org/ifna/e107_files/downloads/lectures/H1LocalAne.pdf) cited on 27 September 2013

**Prof. Dr. Mont Kumpugdee-Vollrath** was born in Bangkok/Thailand. She was graduated Bachelor of Science in Pharmacy in 1993, Faculty of Pharmacy, Mahidol University, Thailand, Master of Sciences in Pharmacy in 1996 from Mahidol University in collaboration with the Institute of Pharmacy, Christian-Albrechts-University of Kiel, Germany, and the Doctoral Degree in Natural Sciences in 2002 from Institute of Pharmacy, Faculty of Chemistry, University of Hamburg, Germany. 2002-2005 Scientist at GKSS Research

Center, Germany. 2004-2005 Part-time lecturer at the Technical University Carolo-Wilhelmina of Braunschweig, Germany. Since 2005 Professor of Pharmaceutical Technology at Beuth Hochschule für Technik Berlin - University of Applied Sciences, Berlin, Germany. Since 2007 Head of Laboratory Chemical and Pharmaceutical Technology. She is reviewer for many journals and funding programs.

**Dr. Tanasait Ngawhirunpat** was born in 2 April 1971 in Bangkok/Thailand. He was graduated Bachelor of Science in Pharmacy in 1993, Master of Sciences in Pharmacy in 1995 from Faculty of Pharmacy, Mahidol University, Thailand, and Doctor of Philosophy (Pharmaceutical Sciences) in 2002 from Faculty of Pharmaceutical Sciences, Toyama and Pharmaceutical University, Japan. Since 2005 Associate Professor of Faculty of Pharmacy at Silpakorn University, Thailand, Since 2008 Associate Dean for Academic Faculty of Pharmacy at Silpakorn University, Thailand.

**Mr. Thirapit Subongkot** has been PhD student at Silpakorn University, Faculty of Pharmacy, Thailand since 2008 granted by the Thailand Research Funds through the Golden Jubilee Ph.D. Program (Grant no.PHD/0057/2551).